Short Communication

Impact on Fuel Transport Efficiency in Anode of Planar Solid Oxide Fuel Cells

Fuxing Miao[*]

School of Mechanical Engineering and Mechanics, Ningbo University, 818 Fenghua Road, Ningbo, 315211, China
[*]E-mail: aifxmiao@gmail.com

This work establishes a mathematical model of fuel transport efficiency in anode that permeates from the surface to the triple phase boundaries through the porous electrode of solid oxide fuel cells. And the relationship between the fuel transport efficiency and the parameters of the porous anode and gas channel is verified with the reported experimental results. The result shows that the fuel transport efficiency in anode is proportional to the porosity of the supported-anode and the length of the gas channel on interconnects. The fuel transport efficiency is also inversely proportional to the porosity and height of the gas channel on interconnect and the thickness of the porous supported-anode. When the porosity of the supported- anode is fixed, the fuel transport efficiency can be improved by reducing the porosity or extending the gas channel length, or reducing the gas channel height on the interconnect, or reducing the thickness of the porous-anode. When the porosity, height, and length of the gas channel on the interconnect are fixed, the fuel transport efficiency in anode can be improved by increasing the porosity or reducing the thickness of the porous anode.

1. INTRODUCTION

Solid oxide fuel cells (SOFCs) are an efficient energy converter whose efficiency can reach above 70%, and is therefore regarded as a new type of power generator for the future [1]. The SOFCs have two types: tubular and planar [2], in which the planar type is particularly favored because of its convenience for large-scale integration. The planar SOFCs are divided into three types based in the support materials, namely, cathode support, electrolyte support, and anode support, where the anode-supported cell is an important research focus because of its low working temperature and high density of output power among other factors [3]. The Ni-YSZ/YSZ/LSM-YSZ type is regarded as the main

anode-supported cell with extensive prospects due to its special requirements on working temperature, environment, and interaction between components [4]. Single cells, due to limited energy, are well known to combine in series or in parallel to a SOFC stack to obtain necessary energy [5]. Hence, the stack is a core component in a SOFC power generation system, and its performance directly determines whether the SOFC power generation system can be commercialized.

To meet the demand for commercialization, specific requirements are imposed on the performance of a SOFC stack. For example, the power density should exceed 0.4 Wcm^{-2} under the working voltage of 0.7 V, the fuel utilization must be ≥70%, and the lifetime should reach 40,000 h [6]. To achieve these targets, researchers have studied the factors affecting the density of output power and the lifetime of a SOFC stack. The result shows that the interface contact between the cell cathode and the metal interconnect is the key factor affecting the density and lifetime of output power [7-9]. Hence, the power density and lifetime of a SOFC stack can be remarkably increased by improving the interface contact between the cathode and the interconnect. However, researchers have found that despite the remarkably improved electrical performance and lifetime of a SOFC stack, its fuel utilization is far less than the requirement of above 70% in most situations. For example, L. Blum et al. [10] reported that the fuel utilization of a stack under the working condition was about 40%, showing a huge gap from the requirements for commercialization.
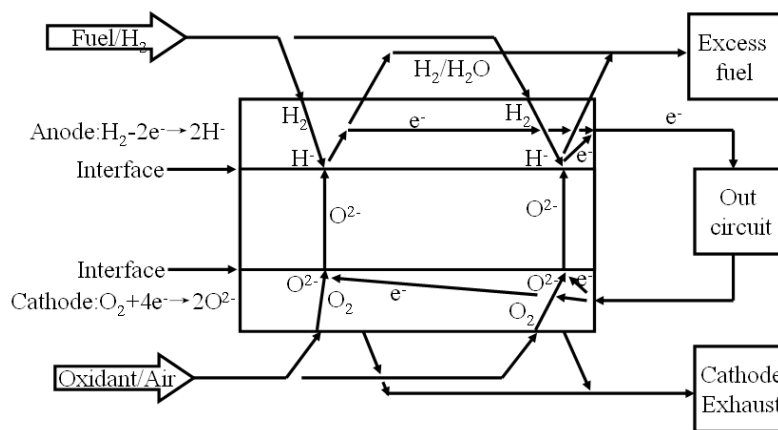

Figure 1. Schematic illustration of the working principle for SOFC

Fig. 1 shows the working principle of SOFCs [11], wherein the fuel diffuses to the triple phase boundaries of the active sites through the support anode, and undergoes oxidation reaction at the triple phase boundaries of the cell anode to produce electrons. The electrons are then transported to the cell cathode through the electronic conductor of the supported-anode and the eternal electronic conductor, finally reaching the triple phase boundaries of the cell cathode, and undergoing a reduction reaction with the gaseous oxidant waiting there. Next, the reduced gaseous oxidant reacts with the fuel gas transmitted through the electrolyte. The working process is repeated, which continuously generates power. Hence, it can be concluded that improving the cell electric performance and the actual fuel utilization is not only related to the improvement of the interface between cell electrodes and interconnects, but also directly related to the permeation of fuel through the anode.

Generally, fuel utilization can be increased to a certain degree along with the increasing electric performance by improving the interface contact to boost the effect of electron collection. However, such means still can't enable fuel utilization to reach the efficiency required for commercialization, which has a direct correlation to the impact on the fuel transport efficiency in supported-anode. As to the Ni-YSZ/YSZ/LSMYSZ type cell, the cell supported material was initially NiO-YSZ with various thickness. For example, Mukhopadhyay et al. [12] reported a thickness of 1.2 mm to 1.5 mm, and Bora et al. [13] reported a thickness of 0.4 mm to 0.6 mm. The structure of SOFC stack is also different. For example, Schuler et al. [14] and Herle et al. [15] adopted a co- flow structure, where the cell active area was 50 cm^2 and the thickness of supported-anode was 0.4 ~ 0.6 mm, Huang et al. [16] adopted a cross-flow structure, where the thickness of supported-anode was 0.55 mm with various cell area, Yokoo et al. [17] adopted an internal flow structure, where the cell active area was 60 cm^2 and the thickness of supported-anode was 1.1 mm. Hence, the flow rate of fuel from the gas channel and the fuel permeating into the triple phase boundaries through the porous supported-anode are various among them, resulting in different fuel utilization and electrical efficiency.

As to the supported-anode planar SOFCs, researchers became aware of the importance of the anode structure on cell performance, and began to improve the electrical performance by adjusting the cell structure, which subsequently improved fuel utilization as well [18-19]. In addition, the fuel utilization, in turn, has a significant influence on cell performance [20]. Hence, researchers conducted numerous simulation studies on fuel gas transport inside the anode, and established a transport model of fuel gas to obtain the mole fraction of gas transport inside the anode under fixed porosity, cell size, and other parameters [21-25]. In addition, they analyzed the fuel gas transport and distribution inside the cell electrode. However, the research on fuel transport efficiency in the porous anode was generally ignored, which imposes limits on the SOFC stack to improve its electrical performance and its actual fuel utilization. Hence, the aim of this work is to establish a mathematical model of the fuel transport efficiency that permeates to the triple phase boundaries from the anode side through the porous electrode, and analyze the factors on fuel transport efficiency on the anode side by comparing it with the published experimental result to further verify the model, which are helpful to provide a reference for adopting measures to improve the electrical performance of SOFCs and its actual fuel utilization.

2. THORETICAL ANALYSIS AND MODELING

Fig. 2 shows the gas transport in a working SOFC. When the gas is fed from the entrance, part of fuel gas is transmitted to the exit through the gas channel of the metal interconnector. During this process, part of gas is permeated to the triple phase boundaries through the porous support-anode and reacts with the oxidant gas. Assuming the Q_x as the flow rate of fuel through the gas channel of the metal interconnect, it can be written as the following based on the literature [26]

$$Q_x = \frac{\varepsilon_x \cdot A_x \cdot D_{effx} \cdot \Delta C_x}{L} \qquad (1)$$

where Q_x is the flow of fuel through the metal interconnector's gas channel, m^{3}s^{-1}, D_{effx} is the effective diffusion coefficient through the cross-section of the metal interconnector's gas channel,

$m^2 s^{-1}$, A_x is the total area of diffusion along the cross-section of the metal interconnector's gas channel, m^2, ε_x is the porosity of gas flowing along the gas channel of the metal interconnector, ΔC_x is the concentration difference between two ends of gas channels on the metal interconnector, L is the gas channel length on the interconnect surface, m.
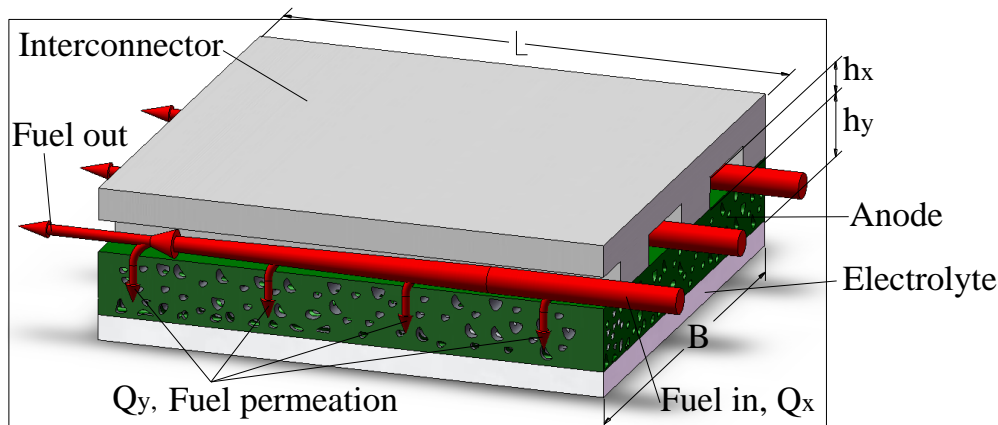

Figure 2. Schematic illustration of the gas transport process

According to the reference reported [27-28], the effective diffusion coefficient in Formula (1) can be expressed as

$$\frac{1}{D_{eff}} = \frac{1}{D_b} + \frac{1}{D_k} \qquad (2)$$

where D_b is the self-bulk diffusion coefficient of gas, $m^2 s^{-1}$, D_k is the Knudsen coefficient.

The size of gas channel on the metal interconnector is normally quite large. Therefore, gas diffuses in the gas channel of metal interconnect are mainly determined by the flow of viscous gas and molecular diffusion, and the Knudsen diffusion may be disregarded [29]. The diffusion coefficient for this work can thus be expressed as

$$D_{eff\,y} = D_b \qquad (3)$$

As illustrated in Fig. 2, the cross-section area in Formula (1) can be expressed as

$$A_x = B \cdot h_x \qquad (4)$$

where B is the width as shown in Fig.2, m, h_x is the gas channel width on the interconnector, m.

Formulas (3) and (4) are substituted into Formula (1), then the gas flow on the gas channel of the metal interconnect can be expressed as

$$Q_x = D_b \cdot \varepsilon_x \cdot B \cdot h_x \cdot \frac{\Delta C_x}{L} \qquad (5)$$

As illustrated in Fig. 2, when gas transports through the gas channel of metal interconnect, part of gas permeates to the triple phase boundaries through the pores. The flow rate that permeates to the triple phase boundaries can be expressed by the formula below [30]

$$Q_y = \frac{\mu \cdot A_y \cdot \Delta P_y}{\eta \cdot h_y} \qquad (6)$$

where Q_y is the flow rate of fuel that permeates to the triple phase boundaries through the porous electrode, $m^3 s^{-1}$, A_y is the total area of diffusion along the cross-section of the porous support-anode, m^2, ε_y is the porosity of the porous anode, ΔP_y is the pressure drop from entrance to exit of the micropores of the porous anode, Pa, h_y is the thickness of the porous anode, m, d is the pore diameter inside the porous anode, m, μ is the permeation coefficient of gas inside the porous electrode, m^2, η is the dynamic viscosity of the gas fluid, Pa s.

The gas permeation parameter can be obtained through the formula below [30]

$$\mu = \frac{d^2}{32} \cdot \varepsilon_y \qquad (7)$$

As illustrated in Fig. 2, the cross-section area in Formula (6) can be expressed as

$$A_y = B \cdot L \qquad (8)$$

By substituting Formulas (7) and (8) into Formula (6), the flow rate of fuel gas through the porous anode can be expressed as

$$Q_y = \frac{d^2 \cdot \varepsilon_y \cdot B \cdot L \cdot \Delta P_y}{32 \cdot \eta \cdot h_y} \qquad (9)$$

Assuming the the flow rate of Q_x is the total flow, based on the above description, the transport efficiency F_u of fuel gas from the porous supported-anode to the triple phase boundaries is

$$F_u = \frac{Q_y}{Q_x} \qquad (10)$$

Hence, the Formula (10), which refers to the fuel transport efficiency, can be expressed as

$$F_u = \frac{d^2}{32 \cdot \eta \cdot D_b} \cdot \frac{\Delta P_y}{\Delta C_x} \cdot \frac{L^2}{h_x \cdot h_y} \cdot \frac{\varepsilon_y}{\varepsilon_x} \qquad (11)$$

Assume

$$\kappa = \frac{d^2}{32 \cdot \eta \cdot D_b} \cdot \frac{\Delta P_y}{\Delta C_x} \qquad (12)$$

Hence, Formula (11) can be simplified as

$$F_u = \kappa \cdot \frac{L^2}{h_x \cdot h_y} \cdot \frac{\varepsilon_y}{\varepsilon_x} \qquad (13)$$

3. RESULTS AND DISSCUSSION

Formula (13) reveals that the transport efficiency F_u of fuel gas that permeates from the porous supported-anode to the triple phase boundaries is proportional to the porosity ε_x and length L of the gas channel of the metal interconnect and inversely proportional to the porosity ε_y of the porous supported-anode, the height h_x of the gas channel of the interconnect, and the thickness h_y of the supported-anode. Hence, the transport efficiency of fuel gas can be improved by two aspects. When the parameters of the gas channel on the metal interconnect remain constant, the transport efficiency of fuel gas can be improved by increasing the porosity of the supported-anode ε_y or by reducing the thickness of the supported-anode h_y. When the porosity ε_y and thickness h_y of the supported-anode

remain unchanged, fuel transport efficiency can be increased by extending the length L of the gas channel on the metal interconnect or by reducing its porosity ε_x.

To verify the theoretical model, the experimental result reported in literature was applied by F. Zhao et al. [31], in which the work investigated the effect of the parameters of the supported-anode on cell performance.
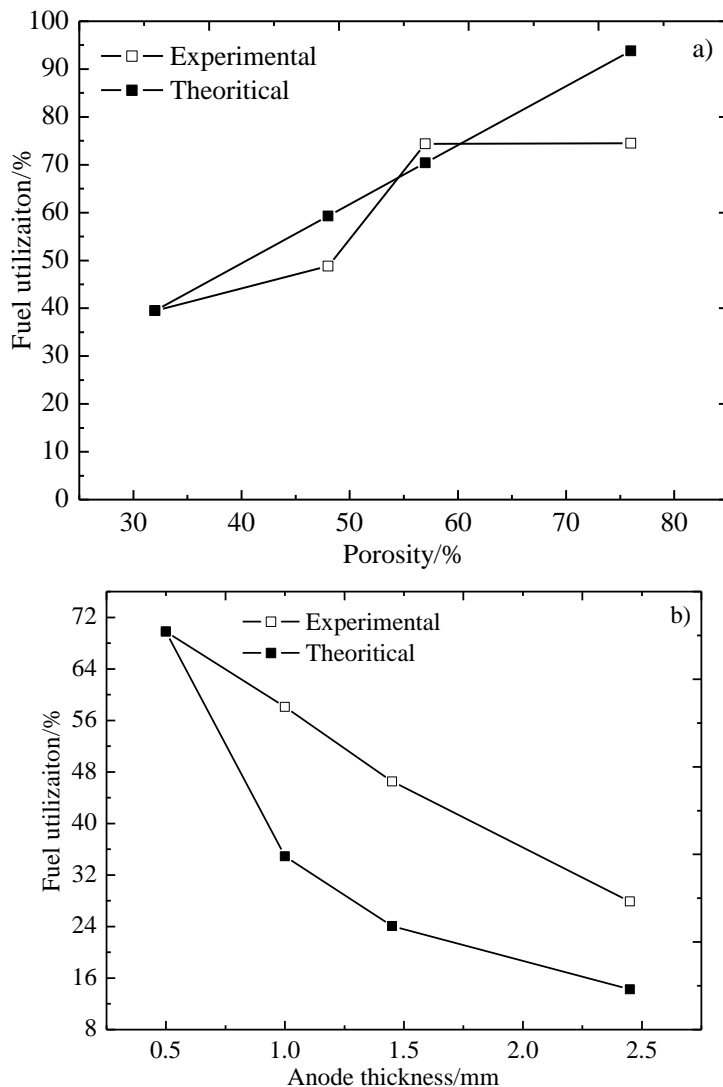

Figure 3. Comparison of the theoretical calculation result and the calculated result in literature

The experimental results show: (1) when other parameters of a single cell are certain, the cell performance under 0.7 V gradually increases from about 0.58 W cm^{-2} to 0.9 W cm^{-2} at 48%, 1.15 W cm^{-2} at 57%, and 1.20 W cm^{-2} at 76% under the same gas flow and working temperature when the porosity of the supported-anode increases from 32% to 48%, 57%, and 76%, respectively. The fuel fed in the experiment was hydrogen at a flow rate of 300 sccm, and the cell active area was 2 cm^2. A preliminary calculation indicated that the fuel utilization was in the sequence of 39.5%, 48.8%, 74.4%, and 74.5% as the porosity increased. (2) when other parameters of the cell anode remain constant, the

output power density of the cell under 0.7 V is in the sequence of 0.58, 0.71, 0.90, and 1.06 W cm^{-2} when the thickness of the cell anode drops from 2.45 mm to 1.45, 1.0, and 0.5 mm, respectively. The formula reported by W. Winkler [32] is applied to calculate the fuel utilization, the value of fuel utilization in the experiment is in the sequence of 27.9%, 46.5%, 58.1%, and 69.8%.

Fig. 3 shows the experimental estimation reported in literature and the theoretical estimation by means of Formula (13). Fig. 3(a) compares the theoretical calculation of the fuel transport efficiency under different porosities of the supported-anode and the actual fuel utilization that resulted from the experiment. The calculation assumes that the theoretical transport efficiency F_u is consistent with the fuel utilization that resulted from the experiment when the porosity is 32%. Since the fuel transport efficiency F_u is linearly proportional to the porosity, the theoretical calculation of F_u is in the sequence of 39.5%, 59.3%, 70.4%, and 93.8% as the porosity increases. The theoretical calculation result of F_u is quite close to the actual fuel utilization when the porosity is 32%, 48%, and 57%, respectively. When the porosity is 76%, the theoretical calculation of F_u deviates more from the actual fuel utilization that resulted from the experiment. F_u in this work indicates the transport efficiency of fuel that permeates from the surface to the triple phase boundaries through the porous electrode. The actual fuel utilization that resulted from the experiment is the efficiency of gas that permeates to the triple phase boundaries as it takes part in the chemical reaction. When the porosity of the support-anode is 76%, the transport efficiency of fuel is much greater than the actual utilization, i.e., the flow rate of fuel gas that permeates to the triple phase boundaries is far more than the flow being utilized in a timely manner. The actual fuel utilization can't be improved further even the fuel transport efficiency is higher due to the limited cell performance. The result also shows that it is unnecessary to increase the porosity further when the fuel utilization has reached its maximum.

Fig. 3(b) compares the theoretical calculation of the fuel transport efficiency under different anode thicknesses and the actual calculation of fuel utilization that resulted from the experiment. Assuming that the fuel transport efficiency F_u is consistent with the actual fuel utilization when the thickness is 0.5 mm, as the thickness increases, the fuel transport efficiency reduces accordingly and becomes smaller than the actual utilization by 23.2%, 22.4%, and 13.7%, respectively, indicating that the big difference between them. It can be deduced that the difference perhaps results from the results that the actual fuel transport efficiency F_u is much higher than the actual fuel utilization when the thickness of anode is 0.5 mm. Assuming that the fuel transport efficiency F_u is consistent with the actual fuel utilization when the thickness is 0.5 mm, the fuel transport efficiency will naturally be lower than the actual fuel utilization with the increasing thickness. However, as the thickness increases, declining trends of the fuel transport efficiency F_u is consistent with that of the actual fuel utilization. Based on Fig. 3(b), when the anode gets thicker, the fuel transport efficiency gets closer to the actual fuel utilization when the porosity is 48%, verifying the theoretical model.

4. CONCLUSIONS

This work built a mathematical model of the fuel transport efficiency of SOFCs that permeates from the cell surface to triple phase boundaries through the porous anode: $F_u = \kappa \cdot \dfrac{L^2}{h_x \cdot h_y} \cdot \dfrac{\varepsilon_y}{\varepsilon_x}$. The result

of this mathematical model indicates that the fuel transport efficiency that permeates to the triple phase boundaries through the porous supported electrode is proportional to the porosity of the support electrode and the length of the interconnector's gas channel, and inversely proportional to the porosity and height of the interconnector's gas channel and the thickness of the porous supported electrode. The actual utilization of SOFC is quite consistent with the trend of the theoretical calculated fuel transport efficiency, which verifies the theoretical model. Hence, the fuel transport efficiency can be increased by reducing the porosity or extending the gas channel length, or reducing the gas channel height on the metal interconnect, or by decreasing the size or increasing the porosity of the porous electrode, which will result in the higher actual fuel utilization.

References

1. S.C Singhal, *Solid State Ionics*, 135(2000)305.
2. N.Q. Minh, *Solid State Ionics*, 174(2004)271.
3. W.Z. Zhu, S.C. Deevi, *Mater. Sci. and Eng. A*,362(2003)228.
4. T. Tsai, S.A. Barnett, *Solid State Ionics*, 93(1997) 207.
5. T.L Wen, D. Wang, H.Y. Tu, M. Chen, Z. Lu, Z. Zhang, H. Nie, W. Huang, *Solid State Ionics*, 152-153(2002)399.
6. J.P.P. Huijsmans, F.P.F. van Berkel, G.M. Christie, *J. Power Sources*, 71 (1998) 107.
7. S.P. Jiang, J.G. Love, L. Apateanu, *Solid State Ionics*, 160(2003)15.
8. W.B. Guan, H.J. Zhai, L. Jin, T.S. Li, W.G. Wang, *Fuel Cells*, 11(2011)445.
9. W.B. Guan, L. Jin, X. Ma, W.G. Wang, *Fuel Cells*, 12(2012)1085.
10. L. Blum, U. Packbier, I. C. Vinke, L.G. J. deHaart, *Fuel Cells*, 2012,DOI: 10.1002/fuce.201200151.
11. N.Q. Minh, *J. Am. Ceram. Soc.*, 76(1993)563.
12. M. Mukhopadhyay, J. Mukhopadhyay, A.D. Sharma, R.N. Basu, *Solid State Ionics*, 233 (2013) 20.
13. B. Timurkutluk, C. Timurkutluk, M.D. Mat, *Int. J. Energy Res.,* 36(2012)1383.
14. J. Andreas Schuler, Z. Wuillemin, A. Hessler-Wyser, C. Comminges, N.Y. Steiner, J. Van herle, *J. Power Sources*, 211 (2012) 177.
15. J. Van herle, D. Perednis, K. Nakamura, S. Diethelm, M. Zahid, A. Aslanides, T. Somekawa, Y. Baba, K. Horiuchi, Y. Matsuzaki, M. Yoshimoto, O. Bucheli, *J. Power Sources*, 182 (2008) 389.
16. C.M. Huang, S.S. Shya, C.H. Lee, *J. Power Sources*, 183 (2008) 205.
17. M. Yokoo, Y. Tabat, Y. Yoshid, K. Hayashi, Y. Nozaki, K. Nozaw, H. Arai, *J. Power Sources*, 178 (2008) 59.
18. Y. Patcharavorachot, A. Arpornwichanop, A. Chuachuensuk, *J. Power Sources*, 177 (2008) 254.
19. M. Mukhopadhyay, J. Mukhopadhyay, A. Das Sharma, R.N. Basu, *Solid State Ionics*, 233 (2013) 20.
20. P. Metzger, K.A. Friedrich, H. Müller-Steinhagen, G. Schiller, *Solid State Ionics*, 177 (2006) 2045.

21. W. Lehnert, J. Meusinger, F. Thom, *J. Power Sources*, 87(2000)57.
22. Y.X. Shi, N.S. Cai, C. Li, *J. Power Sources*, 164 (2007) 639.
23. A.S. Joshi, K.N. Grew, A.A. Peracchio, W.K.S. Chiu, *J. Power Sources*, 164 (2007) 631.
24. M. Garca-Camprub, A.Sa´ nchez-Insa, N. Fueyo, *Chem. Eng. Sci.,* 65 (2010) 1668.
25. W. Kong, H.Y. Zhu, Z.Y. Fei, Z.J. Lin, *J. Power Sources*, 206 (2012) 171.
26. Q. Zheng, J. Xu, B. Yang, B.M. Yu, *Physica A*, 392 (2013) 1557.
27. W.G. Pollard, R.D. Present, *Physical Review*, 73(1948)762.
28. D.Q. Mu, Z.S. Liu, C. Huang, N. Djilali, *Microfluid Nanofluid*, 4(2008) 257.
29. W. Kast, C.R. Hohenthanner, *Int. J. Heat Mass Transfer*, 43 (2000) 807.
30. T. Isobe, Y. Kameshima, A. Nakajima, K. Okada, Y. Hotta, *J. Eur. Ceram. Soc.*, 27 (2007) 53.
31. F. Zhao, A.V. Virkar, *J. Power Sources*, 141 (2005) 79.
32. W. Winkler, *J. Power Sources*, 86 (2000)449.